Intermolecular V-V Energy Transfer in the Photodissociation of Weakly Bound Complexes: A New Experimental Approach

E. J. Bohac and R. E. Miller

Department of Chemistry, University of North Carolina, Chapel Hill, North Carolina 27599

(Received 16 February 1993)

Reported here is a newly developed cw-infrared pump-probe method for studying the vibrational predissociation of weakly bound complexes at the state-to-state level. This method is suitable for studying the wide range of dynamical processes possible in these systems. We discuss preliminary results for two systems, N_2-HF and CO_2-HF, which illustrate the versatility of the method and the richness of the accessible dynamics.

PACS numbers: 34.30.+h, 33.80.Gj, 34.50.Ez, 34.50.Pi

High resolution infrared laser-molecular beam spectroscopy has been shown to be a powerful method for studying weakly bound neutral molecule complexes [1,2]. These studies are providing us with an extensive database for a wide range of such systems. Of particular interest is the fact that, even at the low energies associated with infrared excitation, the weak intermolecular bond can dissociate in a way that is highly nonstatistical [1,3]. Although the vibrational predissociation lifetimes obtained from these spectroscopic studies can provide important insights into the nature of these processes, our understanding of the detailed state-to-state dynamics remains far from complete and information on the final state distributions of the associated photofragments are badly needed. Data of this type are sensitive to the vibrational coupling responsible for predissociation, precisely the area where our understanding of these systems is most tenuous. Unfortunately, a versatile method for obtaining final state distributions for many of these systems has not been available.

In a number of recent publications [4–8] we have demonstrated the utility of a method, based upon the measurement of photofragment angular distributions, that in special cases can provide final internal state distributions. In systems where the final vibrational or rotational density of final states is very low, as in HF dimer [4,5,9], individual fragment states can be resolved in the angular distributions owing to the large differences in their kinetic energy release. The limitation of the approach is that as soon as the density of final states becomes even moderately high, they can no longer be angularly resolved. Under these conditions, the only information that can be obtained from the angular distribution is the average photofragment kinetic energy release.

Although a number of pump-probe methods have been developed that do not suffer from this difficulty [10–12], the visible-UV fluorescence and resonantly enhanced multiphoton ionization (REMPI) detection methods upon which they are based are far from general. Infrared spectroscopy can provide the required generality, since most molecules possess at least one IR allowed vibrational mode. For this reason, the approach taken here is to make use of a second high resolution cw-infrared laser to probe the fragments in a state sensitive manner. Detection is based upon the optothermal technique [13], used in such a way that the fragments can be separated from the parent molecules using the angularly resolved method discussed above [4,5]. The combination of photofragment angular and state resolution is a powerful one that provides us with the versatility needed to study many different systems.

The method is illustrated here by discussing preliminary results obtained for the N_2-HF and CO_2-HF systems. These two complexes are of interest owing to the possibility of observing intermolecular V-V energy transfer associated with their photodissociation. In both cases, the dissociation is initiated by the pump laser, tuned to the HF stretching fundamental of the complex, and the probe laser is used to determine the final state of the HF fragment.

The experimental apparatus developed for this purpose is shown schematically in Fig. 1. Two spherical multipass cells are used to improve the excitation efficiency for both the pump and probe laser transitions. The first laser is tuned to a rovibrational transition in the complex of interest, which leads to the production of fragments scat-

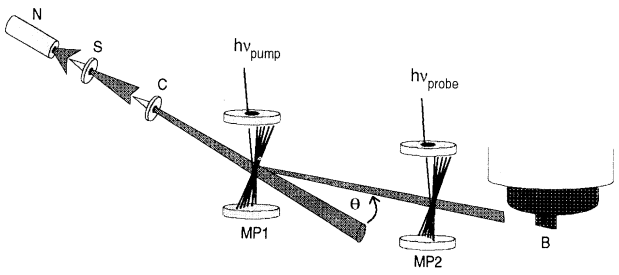

FIG. 1. A schematic diagram of the pump-probe configuration used in the present study. The molecular beam is formed by expanding the gases through a pinhole nozzle, N, and skimming, S, and collimating, C, the resulting expansion. The pump laser is passed through the first multipass cell, MP1, and excites the complex, which fragments into various laboratory angles. The fragments are then probed by the laser passing through the second multipass cell, MP2, and detected by the liquid helium cooled bolometer, B, positioned at angle θ.

0031-9007/93/71(1)/54(4)$06.00

tered to various laboratory angles. These fragments are detected by the liquid helium cooled bolometer. The second F-center laser is tuned to the various monomer fragment transitions to determine their internal state. Excitation of the monomer rovibrational transitions results in an increase in the internal energy of the fragments and a bolometer signal that is proportional to the population in the probed level. For both of the systems considered here, dissociation can only occur if the HF vibration is quenched. As a result, all possible HF fragment states can be probed using the corresponding fundamental rovibrational transitions.

The complexes of interest were formed by expanding a gas mixture composed of 1% HF and 30% N_2 or CO_2 in helium from a source pressure of 400 kPa. With the exception of the modifications needed to introduce the second laser into the chamber, the description of the molecular beam apparatus given elsewhere [5–7] remains valid. Although a number of amplitude modulation schemes can be used in this type of pump-probe experiment to enhance the signal-to-noise ratio, we chose to chop only the pump laser beam, which is locked to an external cavity tuned to the transition frequency of the binary complex. The probe laser, which is not modulated, is then scanned through the various HF transitions. This method has the advantage that the overall fragment signal resulting from the pump laser can be monitored simultaneously with the state selective probe laser signal. This is illustrated in Fig. 2 for the case of the N_2-HF complex, where the bolometer is set at a scattering angle of 6° and the pump laser was tuned into resonance with the $R(4)$ transition of the N_2-HF complex at 3919.3234 cm^{-1} [14]. The probe laser was then tuned through the various HF monomer transitions [$R(0)$, $P(1)$, $P(2)$, . . . , $P(12)$] to determine the population distribution over the available rotational states. Under these conditions, signals were only observed when the probe laser was tuned to the $P(7)$ transition at 3644.1427 cm^{-1} [15].

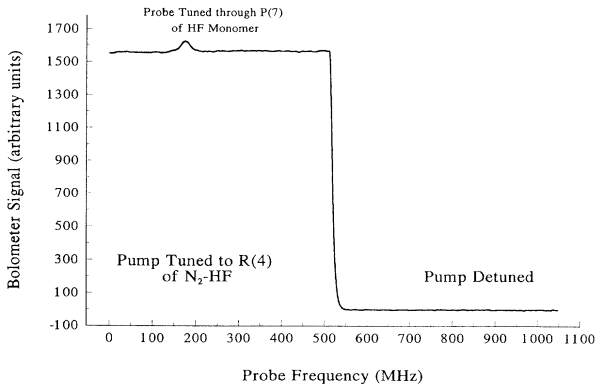

FIG. 2. The pump-probe signals for the case of N_2-HF, obtained at a scattering angle of 6°. The large offset is due to the pump laser signal when tuned to the $R(4)$ transition of N_2-HF. The transition observed on top of this offset results from tuning the probe laser through the $P(7)$ transition of the HF monomer, indicating the presence of HF fragments in the $j=7$ rotational state.

A series of such experiments was then carried out as a function of laboratory scattering angle. At angles beyond 10° the signals associated with the $P(7)$ transition became too weak to observe, even though the total photofragment signal was still significant. A search over the HF monomer transitions at 11° revealed that only the $P(12)$ transition, at 3381.4318 cm^{-1} [15], had measurable intensity. The fact that the $j=12$ channel appears at larger laboratory angles than $j=7$ clearly shows that the translational energy associated with the former is larger than that of the latter. Accounting for the differences in the instrumental response, the probabilities for populating these two states appear to be approximately equal. Considering the high density of fragment channels available in this case, the photodissociation dynamics is clearly very specific. The strong deviations from statistical behavior can provide us with clues concerning the important dynamical pathways, as discussed below.

Despite the fact that the rotational energy associated with the $j=12$ state of HF monomer is 2011.615 cm^{-1} larger than that of the $j=7$ state, the former has the larger kinetic energy release. Since the overall energy must be conserved, the implication is that for $j=7$, a substantial amount of energy is being deposited in another internal degree of freedom of the fragments, the possible candidates being the rotational and vibrational degrees of

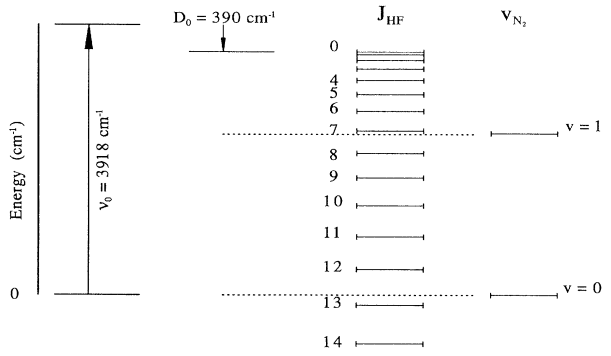

FIG. 3. An energy level diagram for the N_2-HF system. Excitation of the parent complex is represented by the upward pointing arrow. The center portion of the diagram shows that as more energy is deposited in the HF rotational degree of freedom, less is available for N_2 vibration. The $v=0$ and $v=1$ states clearly correlate in energy with the $j=12$ and $j=7$ states of the HF fragment, respectively. This is based upon the estimated intermolecular bond dissociation energy (D_0) of 390 cm^{-1}. The remainder of the excess energy is partitioned between the rotational degree of freedom of the N_2 fragment (not shown in the diagram) and the recoil energy.

freedom of the N_2. The fact that the vibrational frequency of the N_2 fragment is 2329.922 cm^{-1} [16] leads us to conclude that $j=7$ is produced in coincidence with $v=1$ of the N_2 fragment, while $j=12$ correlates with the $v=0$ state of N_2. Further evidence for this is given in Fig. 3, which shows an energy level diagram for the N_2-HF system. The left portion of the diagram shows the excitation of the parent complex. In order for dissociation to occur, some of this excess energy must be used to dissociate the weak intermolecular bond (D_0). The value given in the figure, namely, 390 cm^{-1}, was estimated by considering the necessary kinetic energies for the two channels, in order to account for their positions in the angular distribution. It is clear from the figure that as more energy is deposited into the HF rotational degree of freedom, less is available for the N_2 fragment. Based upon the estimated dissociation energy, $v_{N_2}=0$, $j_{HF}=12$ and $v_{N_2}=1$, $j_{HF}=7$ are both open channels and the kinetic energy available in the former is greater than in the latter, consistent with the experimental results. Rotation of the N_2 fragment is not expected to be a major sink for the excess energy, owing to its relatively small rotational constant. Work is currently under way to fit the angular distributions in order to extract information on the rotational distribution of the N_2 fragment and to better determine a value for D_0. The latter value, which is very difficult to obtain by other methods, will be very useful in making comparisons with *ab initio* calculations.

The dissociation of N_2-HF is clearly a very selective process, which should afford us the opportunity to obtain deeper insights into the associated vibrational dynamics. What is particularly surprising is the fact that both the $v=0$ and $v=1$ N_2 fragment channels are populated with essentially equal probability, even though the terms in the potential energy surface that couple the initial parent states to the final fragment states must be very different. For the case where HF is produced in $j=7$ and N_2 in $v=1$, V-V coupling is clearly important. In contrast, the process leading to the production of $j_{HF}=12$, $v_{N_2}=0$ depends upon V-R coupling, which accesses high j states of the HF fragment. The latter case requires high order anisotropy in the potential surface, while the former depends upon longer range interactions between the two monomer constituents in the complex. King and coworkers [11] have observed similar behavior for the case of the vibrational predissociation of the open shell complex NO-HF, by probing the rotational and vibrational distributions of the NO fragments. Apparently, the open shell character of the NO-HF system is not a significant factor in determining its dynamical behavior.

We now consider the photodissociation of CO_2-HF. The small rotational constant and numerous vibrational modes associated with the CO_2 fragment make the density of final states extremely high for this system, such that there is no hope for obtaining a unique assignment of the final state distribution from the angular distributions alone. Figure 4 shows an energy level diagram for this system, based upon an estimated dissociation energy for the complex of 700 cm^{-1}. Once again, to retain the clarity of the diagram, the rotational states of the CO_2 have been suppressed. Clearly, a range of CO_2 vibrational states are energetically accessible. From the angular distribution associated with this system we know that the translational energy is small and, given that the rotational constant of the CO_2 fragment is also small, these two depositories for the excess energy cannot be very important. As a result, we expect that the final rotational state of the HF fragment will be strongly correlated with the vibrational state of the CO_2 fragment.

In this experiment the probe laser was tuned through the various HF monomer transitions while the pump laser was held fixed on the $R(5)$ transition of the complex. Only a single HF rotational state was observed for this case, namely, $j=6$, probed using the $P(6)$ transition. From Fig. 4 it is clear that $j=6$ of HF monomer is nearly resonant with the (00°1) vibrational level in CO_2 (note that the resonance is dependent upon the value of D_0). The implication seems to be that, of the possible combinations of HF rotation and CO_2 vibration, only this single combination is populated. Ultimately we would like to probe the CO_2 fragment to check this assignment.

The (00°1) vibrational level of CO_2 is special in that its dipole oscillator strength with the ground state is very large. This leads us to consider a simple model for the dissociation, based upon the following intermolecular V-V process:

$$OCO(00°0)-HF(v=1)\rightarrow OCO(00°1)+HF(v=0).$$

The analogous process has been studied previously in col-

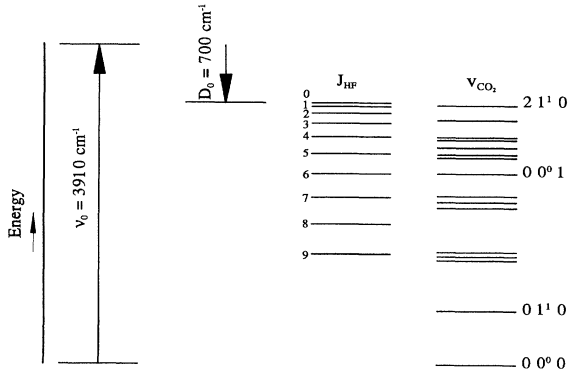

FIG. 4. An energy level diagram for the CO_2-HF system. The dissociation energy (D_0) used in this figure was estimated to be 700 cm^{-1}. The result is a range of CO_2 vibrational states that are energetically available, depending upon the rotational state of the HF fragment. Note that the (00°1) state of CO_2 is very nearly resonant with the $j=6$ state of the HF monomer fragment.

lisions between vibrationally excited HF and ground state CO_2 [17,18]. The results were interpreted using a dipole-dipole model for energy transfer [19,20], which we can adapt for the present case of photodissociation.

We begin by writing the excited state of the parent complex ($\langle i|$) and the photofragment state ($|f\rangle$) as

$$\langle i| = \langle Jmv_{\text{int}}|\langle jk^l m|\langle n|\,,$$

$$|f\rangle = |\text{trans}\rangle|j_{\text{HF}}m_{\text{HF}}\rangle|j_{\text{CO}_2}m_{\text{CO}_2}\rangle|jk^l m\rangle|n\rangle\,,$$

where we have assumed that the vibrational quantum numbers of the monomer units within the complex remain valid. Given that the dipole operator, V', is

$$V' = \frac{\mu_1\mu_2}{r^3}[-2\cos\theta_1\cos\theta_2 + \sin\theta_1\sin\theta_2\cos(\phi_2-\phi_1)]\,,$$

and assuming the intramolecular vibrations are unaffected by the weak van der Waals interactions, the intermolecular parts of the matrix elements connecting the initial and final states can be separated out to obtain

$$P_{if} \propto |\langle 00^\circ 0|Q_{\text{CO}_2}|j'k'^l m'\rangle\langle 1|Q_{\text{HF}}|0\rangle|^2\,.$$

The probability of populating a given final state channel is therefore proportional to the electric dipole transition matrix elements connecting the monomer states involved, namely, HF ($v=0\leftarrow 1$) and the relevant CO_2 vibrational channels. The preference for populating the ($00^\circ 1$) state can now be understood in this simple picture, based upon the extremely large transition moment associated with the ν_3 mode of CO_2. The fact that the ν_2 bend is not an important V-V channel may be indicative of the fact that the associated transition moment is orthogonal to that of the HF stretch and therefore is not strongly coupled to the initial state.

Returning to the N_2-HF system we note that the electric dipole matrix element associated with the $v=1\leftarrow 0$ transition in the isolated N_2 molecule is zero. As a result, the simple dipole-dipole mechanism used to discuss the V-V transfer in CO_2-HF cannot explain the $v=1$ channel in N_2-HF. Nevertheless, by including higher order multipole or induction terms in this treatment, such as dipole-quadrupole and dipole-induced dipole, respectively, nonzero matrix elements can be found. However, since these higher order terms are expected to be smaller than the favorable dipole-dipole terms, we might expect that the probability of populating the $v=1$ state will be much lower in this case, thus allowing the less favorable V-R channel, which leads to the production of N_2 $v=0$, to compete. This may be the explanation for why we observe both the $v=0$ and $v=1$ channels for N_2-HF, while for CO_2-HF the ($00^\circ 1$) channel dominates over all others.

It is obviously premature to suggest that we have identified the mechanisms for energy transfer in these systems, based on this simple model. Indeed, more sophisticated theories will undoubtedly be necessary to account for all of the important details, including rotation. Nevertheless, the main point of the present Letter is that we now have an experimental method that can provide the data necessary to test this and other models on a wide variety of systems. Work is presently under way to use these data, together with the translational distributions obtained from the angular distributions, to obtain more complete final state descriptions of these two systems, including intermolecular scalar correlations and vector correlations, as well as dissociation energies.

Support for this research from the National Science Foundation (Grant No. CHE-89-00307) and the Donors of the Petroleum Research Fund (administered by the ACS) is gratefully acknowledged. E.J.B. is grateful for fellowships from the Department of Education and the Hercules Foundation. We are grateful to Professor Brian J. Orr for several helpful discussions.

[1] R. E. Miller, Science **240**, 447 (1988).
[2] D. J. Nesbitt, Chem. Rev. **88**, 843 (1988).
[3] Z. S. Huang and R. E. Miller, J. Chem. Phys. **90**, 1478 (1989).
[4] D. C. Dayton, K. W. Jucks, and R. E. Miller, J. Chem. Phys. **90**, 2631 (1989).
[5] E. J. Bohac, M. D. Marshall, and R. E. Miller, J. Chem. Phys. **96**, 6681 (1992).
[6] E. J. Bohac and R. E. Miller, J. Chem. Phys. **98**, 2604 (1993).
[7] E. J. Bohac, M. D. Marshall, and R. E. Miller, J. Chem. Phys. **97**, 4890 (1992).
[8] E. J. Bohac, M. D. Marshall, and R. E. Miller, J. Chem. Phys. **97**, 4901 (1992).
[9] M. D. Marshall, E. J. Bohac, and R. E. Miller, J. Chem. Phys. **97**, 3307 (1992).
[10] M. P. Casassa, J. C. Stephenson, and D. S. King, J. Chem. Phys. **89**, 1966 (1988).
[11] J. H. Shorter, M. P. Casassa, and D. S. King, J. Chem. Phys. **97**, 1824 (1992).
[12] Y. Rudich and R. Naaman, J. Chem. Phys. **96**, 8616 (1992).
[13] T. E. Gough, R. E. Miller, and G. Scoles, Appl. Phys. Lett. **30**, 338 (1977).
[14] K. W. Jucks, Z. S. Huang, and R. E. Miller, J. Chem. Phys. **86**, 1098 (1987).
[15] D. Goddon, A. Groh, H. J. Hanses, M. Schneider, and W. Urban, J. Mol. Spectrosc. **147**, 392 (1991).
[16] G. Herzberg, *Molecular Spectra and Molecular Structure I. Spectra of Diatomic Molecules* (Van Nostrand Reinhold, New York, 1950), 2nd ed., pp. 1–658.
[17] J. K. Hancock and W. H. Green, J. Chem. Phys. **57**, 4515 (1972).
[18] G. M. Jursich, D. R. Ritter, and F. F. Crim, J. Chem. Phys. **80**, 4097 (1984).
[19] T. A. Dillon and J. C. Stephenson, J. Chem. Phys. **58**, 2056 (1973).
[20] R. T. Pack, J. Chem. Phys. **72**, 6140 (1980).

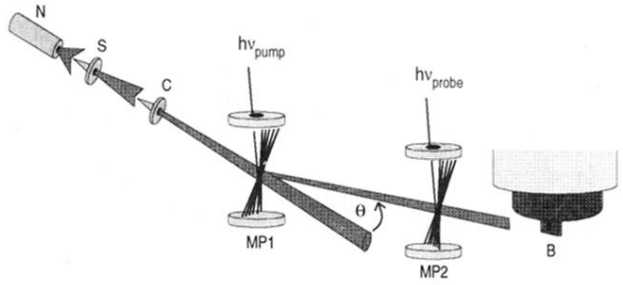

FIG. 1. A schematic diagram of the pump-probe configuration used in the present study. The molecular beam is formed by expanding the gases through a pinhole nozzle, N, and skimming, S, and collimating, C, the resulting expansion. The pump laser is passed through the first multipass cell, MP1, and excites the complex, which fragments into various laboratory angles. The fragments are then probed by the laser passing through the second multipass cell, MP2, and detected by the liquid helium cooled bolometer, B, positioned at angle θ.